JTTEE5 18:665–671
DOI: 10.1007/s11666-009-9350-1
1059-9630/$19.00 © ASM International

Thermo-Physical Properties and Thermal Shock Resistance of Segmented $La_2Ce_2O_7$/YSZ Thermal Barrier Coatings

Hongbo Guo, Yi Wang, Lu Wang, and Shengkai Gong

(Submitted March 8, 2009; in revised form June 1, 2009)

$La_2Ce_2O_7$ (LCO)/yttria-stabilized zirconia (YSZ) thermal barrier coating (TBC) with segmentation crack structure was produced by atmospheric plasma spraying. Thermo-physical properties, such as thermal diffusivities and thermal conductivities, and thermal cycling performance of the segmented LCO/YSZ TBC were investigated. The thermal conductivity of the segmented coating was measured to be around 1.02 W/mK at 1200 °C, relatively lower than that of the non-segmented coating, respectively. The segmented LCO/YSZ TBC exhibited a thermal cycling lifetime of around 2100 cycles, improving the durability by nearly 50% as compared to the non-segmented TBC. The failure of the segmented coating occurred by chipping spallation and delamination cracking within the coating.

Keywords $La_2Ce_2O_7$ (LCO), segmentation cracks, thermal barrier coatings (TBCs), thermal shock, thermo-physical properties

1. Introduction

Thermal barrier coatings (TBCs) have been extensively used in hot section components of gas turbines to increase turbine inlet temperature (TIT) with a consequent improvement in engine efficiency or to improve significantly the durability of the hot components (Ref 1, 2). TBC system typically consists of an oxidation-resistant metallic bond coat and a ceramic top coat as thermal barrier. In total, 7-8 wt.% yttria-stabilized zirconia (YSZ) has been widely used as a standard TBC material since the last decades. For next generation of advanced engines, further increase in thrust-to-weight ratio will require even higher gas TIT. As the result, the TBC materials with higher temperature capability and better thermal insulation performance are in demand. To further increase the operation temperature of turbine components, great efforts have been dedicated to develop new TBC materials to replace the present YSZ. The selection of the TBC materials is restricted by some requirements such as low thermal conductivity, excellent phase stability between room temperature and operating temperature, good resistance to sintering at high temperatures.

Hongbo Guo, Yi Wang, Lu Wang, and **Shengkai Gong**, Department of Materials Science and Engineering, Beijing University of Aeronautics and Astronautics (BUAA), Xueyuan Road, No. 37, Beijing 100191, China. Contact e-mail: guo.hongbo@buaa.edu.cn.

At present, some candidate materials for TBC application at higher temperature are under investigation, such as $LaMgAl_{11}O_{17}$, 7.5 mass% Y_2O_3-HfO_2 (YSH), $Gd_2Zr_2O_7$, $La_2Zr_2O_7$, $La_2Ce_2O_7$ and complex perovskites (Ref 3-7). $La_2Ce_2O_7$ is a promising candidate material for TBC because of its higher phase stability up to 1400 °C, lower thermal conductivity and larger thermal expansion coefficient than YSZ (Ref 8-10). However, thermal cycling performance of the plasma sprayed LCO coating needs improvement in order to make fully use of the potential advantages of the TBC. Recently, segmented YSZ TBCs sprayed at ''hot condition'' have exhibited a promising potential in improving thermal cycling lifetime of TBCs, because the segmentation cracks formed in the TBC during spraying significantly increase the strain tolerance of TBC (Ref 11).

The objective of the present work is to produce LCO/YSZ TBCs with segmentation crack structure while remaining the stoichiometric composition of the sprayed coatings. The effects of the sprayed structures on the thermo-physical properties such as thermal diffusivities and conductivities are concerned. The thermal cycling performances of the non-segmented TBC and segmented TBC are compared and the failure mechanism of the segmented TBC is investigated.

2. Experimental Procedures

2.1 Preparation of LCO TBCs

Powders used for synthesis of LCO included La_2O_3 (99.99%, Grirem Advanced Materials Co., Ltd., China) and CeO_2 (99.99%, Grirem Advanced Materials Co., Ltd., China). The details for the synthesis of LCO have been described in previous work (Ref 8, 10). Commercial NiCoCrAlY powders with a chemical composition of

Ni-21Co-17Cr-12Al-1Y (in wt.%) were chosen for spraying the bond coats of TBCs. The LCO powder for spraying was produced by dried spraying technology. Considering preferential evaporation of components of the feedstock in plasma flame, the mixture ratio of La_2O_3 to CeO_2 for synthesis of LCO was optimized to be 0.4 mole in order to obtain the sprayed LCO coating with nearly stoichiometric composition.

The LCO TBCs were produced by plasma spray with Sulzer Metco plasma spray units. Vacuum plasma spraying with an F4 gun was used to deposit a 120-150 μm NiCoCrAlY bond coat onto disk-shaped Ni-based superalloy substrate. The substrate had a diameter of 30 mm and a thickness of 3 mm. LCO coatings were atmospheric plasma sprayed onto the NiCoCrAlY coated superalloy substrates. Segmentation cracks were generated by thermal tensile stresses during the deposition. The heat input to the substrate should be high enough to obtain a good bonding between lamellae, which is necessary for propagation of vertical cracks from one lamella to the next lamella and finally to the coating surface (Ref 12). Following these ideas, short spray distance, high plasma power and substrate preheating were used. The parameters used for spraying LCO TBCs are listed in Table 1. In the previous work, the LCO TBC had a very poor thermal cycling performance because the LCO coating was not chemically stable with the underlying thermally grown oxides (TGO) mainly consisting of Al_2O_3 (Ref 13). Considering this, a LCO/YSZ double ceramic layer TBC was proposed and exhibited much improved thermal cycling performance. In this work, the LCO/YSZ TBC with segmentation crack structure was also produced, in which YSZ coating was first sprayed as the bottom ceramic layer and LCO coating then deposited onto the YSZ layer. The parameters for spraying LCO/YSZ TBCs are also given in Table 1.

The sprayed specimens were impregnated with epoxy and then sectioned, ground and polished. The planar section and cross section of the coatings were examined by optical microscope (OM) and scanning electron microscope (SEM), the compositions of the coatings analyzed by energy dispersive spectroscopy (EDS). Segmentation crack density was defined as the number of segmentation cracks in a cross section of coating divided by the length of cross section.

2.2 Evaluations of Thermo-Physical Properties

Free-standing LCO coating specimens were produced by removing the LCO coatings from the substrates using chemical etching. Thermal diffusivity $a(T)$ experiments were conducted using a laser flash device (LFA 427/7/G, Netzsch) on disk-shaped specimens of 12.6 mm in diameter and 1 mm in height. Specific heat $C_P(T)$ was determined by using differential scanning calorimeter (DSC, STA 429, Netzsch). The bulk density of the sprayed coating was measured using Archimedes method. For the bulk density measurement, the dry free-standing coating specimen was weighed in air to be W_1, and then soaked in boiling water for 2 h. The specimen was hung up in water and weighed to be W_2. After that, the wet specimen was taken out of water and weighed in air to be W_3. The bulk density ρ was calculated using the equation: $\rho = \frac{W_1}{W_3 - W_2}$. Thermal conductivities $K(T)$ were calculated using the equation: $K(T) = \alpha(T) \times C_P \times \rho$.

Table 1 Processing parameters for spraying $La_2Ce_2O_7$ coatings

Coating	Power, kW	Distance, mm	Ar (slpm)/ H_2 (slpm)	Feed rate, g/min	Gun velocity, mm/s
A	40.2	75	45/10	35-40	400
B	45	65	45/12	35-40	400
C-LCO	40.2	75	45/10	35-40	400
D-LCO	45	65	45/12	35-40	400
C/D-YSZ	40.2	60	45/12	35-40	500

2.3 Thermal Shock Testing

Thermal shock testing of the sprayed LCO TBC specimens was performed in a gas burner test facility. The sample was heated for 20 s to the desired surface temperature of 1250 °C and held at this temperature for 5 min. The surface temperature was measured using a single-color pyrometer (Raytech, Model: 3I2ML3, USA) operated at a wavelength of 0.95-1.1 μm. The measurement was calibrated in order to minimize the effect of emission and reflection.

During heating stage the backside of the sample was cooled by compressed air to maintain a controlled temperature gradient through the sample thickness and, in this case, the substrate temperature was in the range of 950-1000 °C. During cooling stage the burner was removed from the coating surface and the sample cooled by compressed air from both sides for 2 min .The lifetime is defined as the number of thermal cycles at which spallation of around 15% coating surface area occurs.

X-ray photoelectron spectroscopy (XPS) was used to determine the oxidation state of cerium in the coatings. Specimens were analyzed using a Physical Electronics model PHI-5300 XPS system.

3. Results and Discussion

3.1 Microstructure and Phase of Sprayed LCO Coatings

Figure 1(a)-(d) shows the SEM micrographs of cross sections of sprayed LCO coatings as listed in Table 1, respectively. Coatings A and B are single LCO layer TBC. Coating A is porous and contains very few segmentation cracks. The LCO layer thickness is about 150 μm. In contrast to coating A, coating B is relatively denser and reveals segmented structure, in which segmentation cracks went through the whole LCO coating. The segmentation crack density is measured to be 9.5 mm^{-1}. Besides, some branching cracks (horizontal direction) were present together with the segmentation cracks, as marked by arrows. Both coatings C and D are double ceramic layer structures, where a 80 μm thickness YSZ was deposited

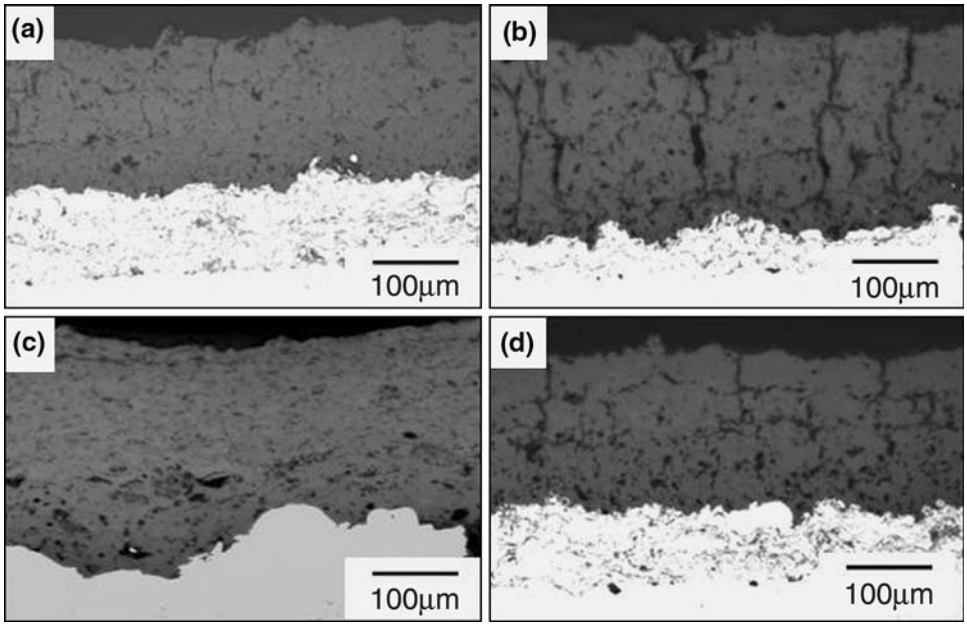

Fig. 1 SEM micrographs of cross sections of the sprayed LCO coatings: (a) traditional structure LCO, (b) segmented LCO, (c) double ceramic layer LCO, and (d) segmented double ceramic layer LCO

as the bottom ceramic layer, while a LCO layer with the nearly same thickness as the top ceramic layer, as shown in Fig. 1(c) and (d), respectively. Coating C reveals a non-segmented structure, whereas coating D a typical segmented structure and its segmentation crack density is about 6 mm^{-1}. Simultaneously, the branching cracks observed in coating B are also formed in coating D. In our previous work, single LCO TBC reacted with the underlying TGO layer mainly consisting of Al_2O_3, which deteriorated the integrity of TBC system at high temperature and led to very short thermal cycling lifetime (Ref 14). The LCO/YSZ double ceramic layer structure has been proved to be chemically stable with the TGO layer and yields a significant improvement in thermal cycling lifetime as compared to the single LCO TBC.

Figure 2(a), (b) and (c) shows the XRD patterns of the LCO powders and the sprayed coatings, respectively. Both the non-segmented and segmented LCO coatings remained single $La_2Ce_2O_7$ phase of a fluorite-type structure (Ref 15). This indicates that decomposition of LCO coating did not occur during thermal spraying. The chemical compositions of the sprayed coatings are determined by EDS, as shown in Table 2. Both of the coatings have a chemical composition close to the stoichiometric composition of $La_2Ce_2O_7$, despite there is a little derivation in the composition. This indicates that the LCO coatings with a nearly stoichiometric composition were obtained under the present plasma spray conditions.

Partial decomposition of LCO usually occurs during plasma spraying or electron beam physical vapor deposition, due to different vapor pressures of La_2O_3 (8×10^{-5} atm, 2500 °C) and CeO_2 (2×10^{-2} atm, 2500 °C), which tends to cause composition derivation of the sprayed LCO coating from the original LCO powders. In viewing of this, it is necessary to consider the design of chemical composition of original powders. In the present work, the ratio of La_2O_3 and CeO_2 powders was optimized in order to spray the LCO coating with a nearly stoichiometric composition.

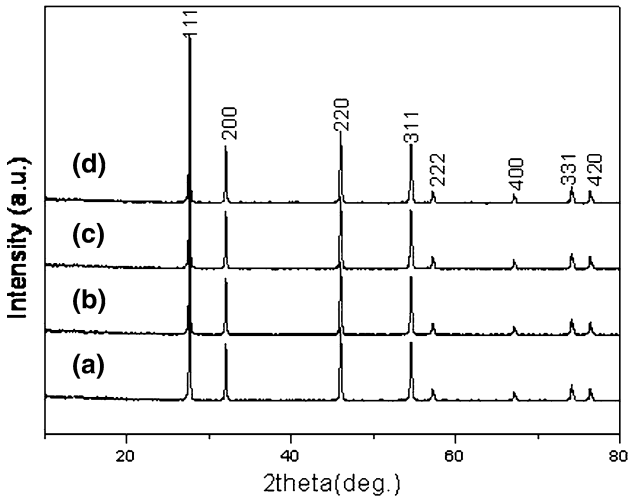

Fig. 2 XRD patterns of the LCO (a) powders, (b) the non-segmented LCO coating, (c) the segmented LCO coating, and (d) segmented double ceramic layer LCO/YSZ after thermal cycles

Table 2 Chemical compositions of sprayed LCO coatings (in at.%)

Coating	La	Ce	O
A	21.85	20.08	58.08
B	23.99	20.52	55.49

It is well recognized that a high heat input to the substrate is required in order to generate high segmentation crack density in the sprayed coating (Ref 16). In this study, a ''hot'' spraying condition, including higher plasma power, shorter spray distance and higher substrate temperature, was used for spraying coatings B and D with segmentation cracks. Due to optimization of the chemical compositions of the original powders and spray parameters, the coatings B and D with the segmentation crack structure were produced, while keeping the stoichiometric composition and single LCO phase.

Substrate temperature has an important impact on the structure features of the sprayed coatings such as segmentation cracks. It is established that high substrate temperature gave rise to a high segmentation crack density (Ref 16). The segmentation cracks originate from the microcracks existing in the initially deposited splats as a result of release of tensile stresses during solidification of the deposited liquid phase. When the spraying was performed at a high substrate temperature, the temperature between two adjacent splats could be high enough to lead to a good splat contact partially by remelting of the surface of the underlying splats. Thus, the tensile stresses generated in the recently deposited splats will be relaxed by propagation of microcracks in the previously deposited splats. Following this procedure, the microcracks will finally go through the coating and finally develop into segmentation cracks. On the contrary, at low substrate temperature, the contact area between splats will be very limited. As a result, a large amount of interlamellar gaps or horizontal cracks will exist in the coating. These cracks or gaps will lead to a significant stress relaxation. In such case, the microcracks in the individual splats could not propagate into segmentation cracks.

3.2 Thermo-Physical Properties of LCO

Figure 3(a) shows the results of thermal diffusivity measurements. The values of thermal diffusivity for the coatings A (non-segmented) and B (segmented) are in the range of 0.2-0.45 $mm^2\ s^{-1}$(between 200 and 1200 °C). The calculated thermal conductivity is given in Fig. 3(b). For coating A, the thermal conductivities are in the range of 0.8-1.3 W/mK, while those for coating B in the range of 0.8-1.1 W/mK. Specifically, at 1200 °C, which is a temperature relevant for TBC application, the conductivity for the coating B is around 1.0 W/mK, slightly higher than that for coating A.

Thermal conductivities of a thermally sprayed coating depend on the coating microstructure. Plasma-sprayed TBCs exhibit a two-dimensional microcrack network: one is horizontal, corresponding to nonperfect contacts between intersplats; the second one is oriented vertically, which mainly results from the microcracking of splats during cooling. It is the horizontal cracks that are particularly effective in reducing the thermal conductivity of the sprayed coating as the interfaces formed by such cracks are perpendicular to the primary heat flux. In addition, dispersed micro-porosity also lowers the thermal conductivity. Among the above coatings, coating B has large

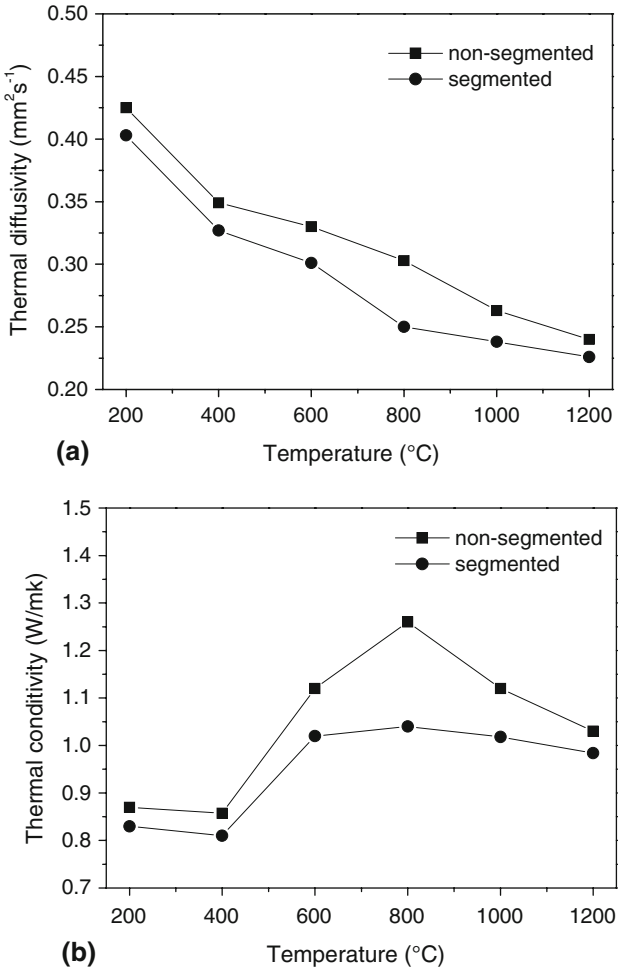

Fig. 3 Thermal diffusivities (a) and thermal conductivities (b) of as-sprayed LCO coatings

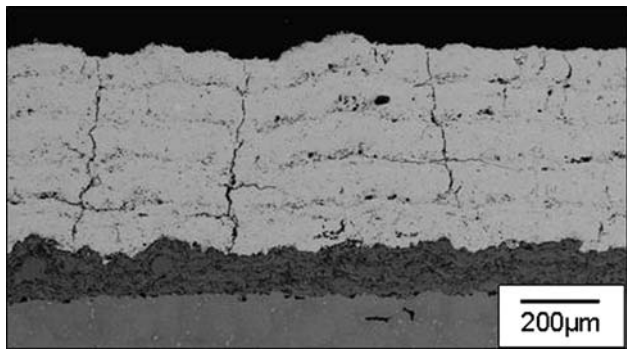

Fig. 4 SEM micrographs of cross sections of the sprayed thick LCO coatings

numbers of horizontal cracks compared to coating A, as shown in Fig. 4, which is beneficial to reducing the thermal conductivity of TBC.

Heat-treatment of the free-standing LCO coating B (segmented) specimen was conducted at 1250 °C and

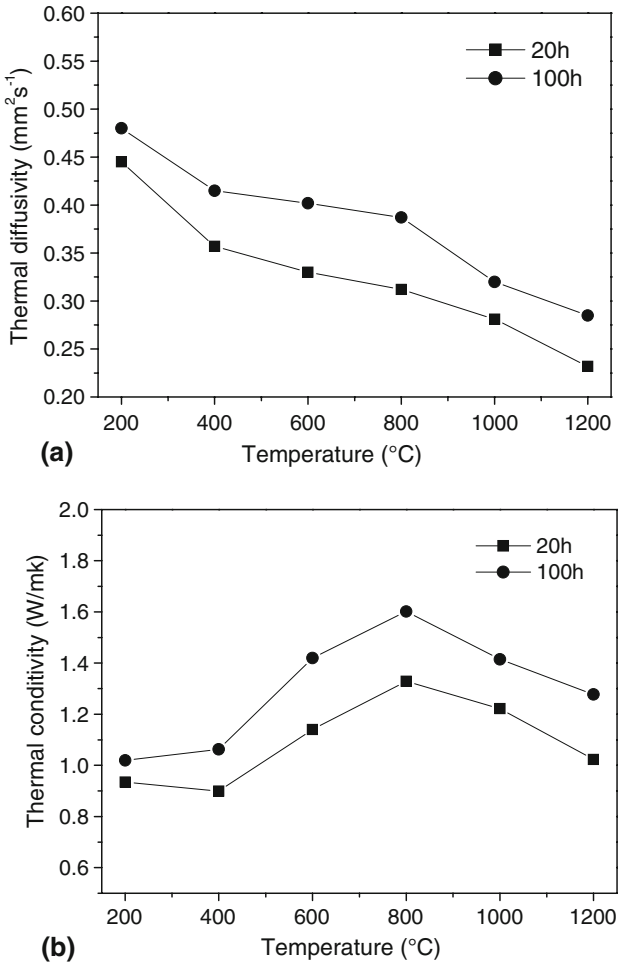

Fig. 5 Thermal diffusivities (a) and thermal conductivities (b) of LCO coatings after 20 and 100 h heat treatment at 1250 °C

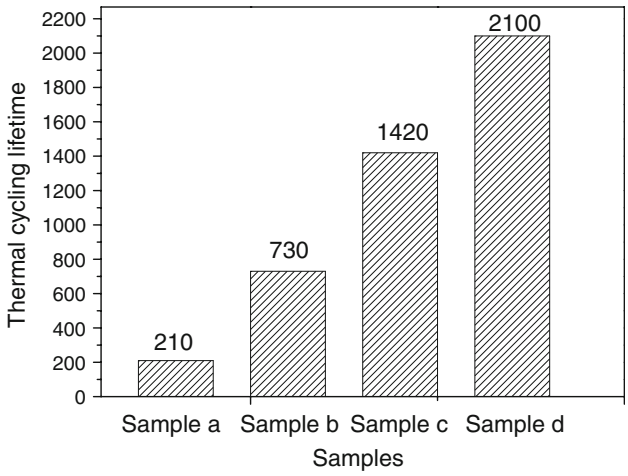

Fig. 6 Thermal cycling lifetime of LCO TBCs: (a) segmented LCO, (b) non-segmented LCO, (c) non-segmented LCO/YSZ, and (d) segmented LCO/YSZ

the thermo-physical properties of the specimen after heat-treatment were concerned. Heat treatment causes an apparent increase in the thermal diffusivity and conductivity of the LCO coating, as shown in Fig. 5. For the coating after 100 h heat treatment, the diffusivity and conductivity at 1200 °C is approximately 0.3 $mm^2 s^{-1}$ and 1.3 W/mK, respectively. Compared to that before heat treatment, the thermal conductivity was improved by nearly 30%. After thermal cycling, most of the micropores disappeared due to the effect of the sintering. Sintering process of plasma sprayed TBC materials usually consists of two separate phases. The first, mainly occurring at very early stage, is characterized by the improvement of intersplat bonding attributed to microcrack healing and by the trans-splat grain growth. The latter sintering quasi-stationary stage promotes mainly the change of pore shape and the reduction of macro-pore volumes (Ref 17).

3.3 Thermal Shock Performance

Coatings A, B, C and D were tested under thermal shock condition and the thermal cycling results are shown in Fig. 6. For the single LCO TBC without segmentation cracks, spallation failure occurred after about 200 cycles at 1250 °C (surface temperature)/950 °C (substrate temperature). The segmented LCO TBC yielded a lifetime of around 700 cycles, which is at least twice higher than that of the non-segmented coating. This indicates that the segmentation crack structure effectively gave rise to improve the thermal shock resistance of TBC.

It should be noted that in the case of the LCO/YSZ double ceramic layer TBCs, both the segmented and non-segmented coatings exhibited much improved lifetime as compared to the LCO single layer TBC. For the non-segmented coating (coating C), the lifetime is about 1400 cycles, while that of the segmented coating was further improved to 2100 cycles. It is clear that even for the double ceramic layered TBC, the segmented structure formed in the coating is also helpful to prolong the TBC lifetime.

For the LCO single layer TBC, the lower thermal shock resistance could be attributed to the chemical reaction of the LCO layer and the underlying TGO mainly consisting of Al_2O_3. It is evident that the chemical reaction degrades the interface bonding between the LCO and TGO layer and leads to spallation of TBC (Ref 18, 19). The strain energy for cracking increases with increasing the volume of a coating which is proportion to the coating. Segmentation cracks in TBCs tend to lower the strain energy for cracking and greatly improve the strain tolerance of the TBC in a manner which behaves like the columnar structure in PVD coatings. Therefore, the segmented TBCs have exhibited a prolonged thermal cycling lifetime as compared to the non-segmented TBCs.

Spallation failure is visible along the specimen rim, as shown in Fig. 7, which is a typical failure mechanism for TBC, resulting from the singularity of thermal stresses at the rim. Figure 8(a) and (b) shows the cross sections of the center part and the edge of the coating D after 2100 thermal cycles, respectively. In the coating center, chipping spallation can be observed, whereas large spallation

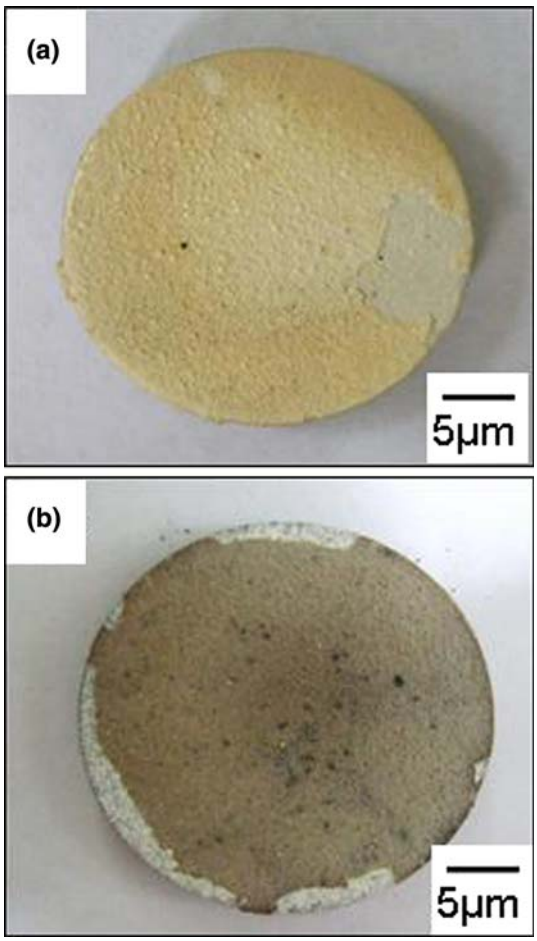

Fig. 7 Photograph of thermal cycling at 1250 °C (surface)/ 1000 °C (bond coat): (a) traditional structure double ceramic layer LCO/YSZ; (b) segmented double ceramic layer LCO/YSZ

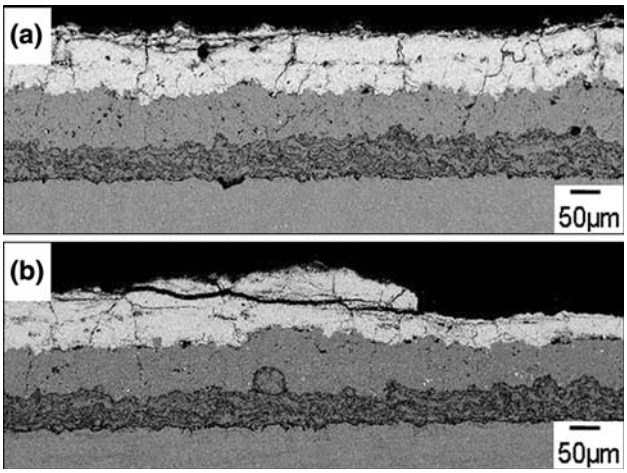

Fig. 8 SEM micrograph of cross section of segmented double ceramic layer LCO/YSZ TBC after 2100 cycles: (a) the center of coating; (b) the edge of coating where chipping occurred

did not occur. In the rim area, spallation caused by delamination cracking occurred at the interface between the first lamellae and the adjacent lamellae, which is a

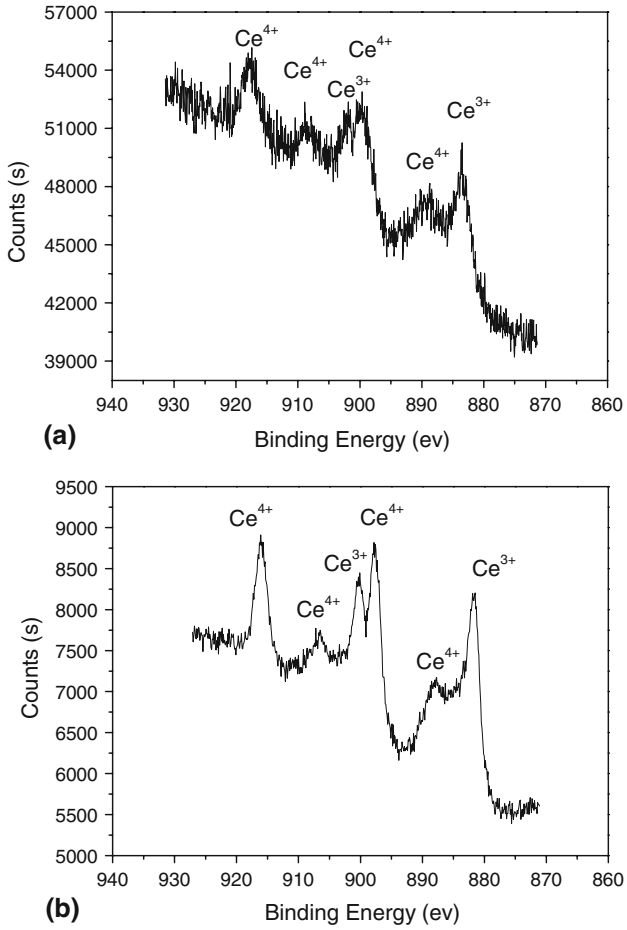

Fig. 9 Ce 3d XPS spectra for the Ce conversion coating

usual failure mode for plasma sprayed TBCs (Ref 19-21). It should be noted that oxidation of bond coat did not dominate the thermal cycling lifetime, since the substrate temperature is not high enough and the total oxidation time not long enough to form a thick TGO layer.

Sintering could be responsible for chipping spallation of the coating. During thermal shock testing, the surface of the LCO layer was exposed to extremely high-temperature gas and caused sintering. Sintering could deteriorate strain tolerance of the coating. On the other hand, partial decomposition could happen. Perhaps, the decomposition phase was too little to be identified by XRD.

Figure 9(a) and (b) shows XPS spectra of the surfaces of coating D before and after the thermal cycling test. Both in the coatings before and after thermal cycling, the Ce 3d spectra have several components with binding energies characteristic of Ce^{3+} and Ce^{4+}. This indicates that the sprayed coating contained both Ce^{3+} and Ce^{4+} species and confirms that a little decomposition occurred during plasma spraying. However, in terms of XRD result as shown in Fig. 2, only LCO single phase was present in the as-sprayed coating. Probably, the decomposition is very limited, which could not be identified by XRD. For the case after thermal shock testing, the coating

surface was exposed to high-temperature flame, which could cause decomposition of the coating. Partially due to the decomposition, chipping spallation occurred.

4. Conclusions

The double ceramic layer LCO thermal barrier coating containing segmentation cracks was produced under ''hot'' spray condition, while remaining phase stability and nearly stoichiometric composition. The segmentation crack density was measured to be around 9.5 mm^{-1}. The segmented double ceramic layer LCO TBC exhibited a thermal cycling lifetime of around 2100 cycles, improving the durability by nearly 50% as compared to the non-segmented TBC. The failure of the segmented coating occurred by chipping spallation and delamination cracking within the coating. The thermo-physical properties of the LCO TBC were evaluated. The thermal conductivity and thermal diffusivity for the segmented coating was measured to be around 1.02 W/mK and 0.238 $mm^2 s^{-1}$ at 1200 °C, relatively lower than those of the non-segmented coating, respectively. Heat treatment caused an increased thermal conductivity due to sintering effect.

Acknowledgments

This research is sponsored by national natural science Foundation of China (NSFC, NO. 50771009 and NO. 50731001) and program for Changjiang scholars and innovative research team in university (PCSIRT) (IRT0512).

References

1. F. Cernuschi, P. Bianchi, M. Leoni, and P. Scardi, Thermal Diffusivity/Microstructure Relationship in Y-PSZ Thermal Barrier Coatings, *J. Therm. Spray Technol.*, 1999, **8**, p 102-109
2. R.A. Millller, Thermal Barrier Coatings for Aircraft Engines: History and Directions [J], *J. Therm. Spray Technol.*, 1997, **6**, p 35-42
3. R. Gadow and M. Lischka, Lanthanum Hexaaluminate-Novel Thermal Barrier Coatings for Gas Turbine Applications-Materials and Process Development, *Surf. Coat. Technol.*, 2002, **392**, p 392-399
4. K. Matsumoto, Y. Itoh, and T. Kameda, EB-PVD Process and Thermal Properties of Hafnia-Based Thermal Barrier Coating, *Adv. Mater.*, 2003, **4**, p 153-162
5. R. Vassen, X. Cao, F. Tietz, D. Basu, and D. Stöver, Zirconates as New Materials for Thermal Barrier Coatings, *J. Am. Ceram. Soc.*, 2000, **83**, p 2023-2028
6. R. Vassen, A. Stuke, and D. Stöver, Recent Developments in the Field of Thermal Barrier Coatings, *J. Therm. Spray Technol.*, 2009. doi:10.1007/s11666-009-9312-7
7. M.O. Jarligo, D.E. Mack, R. Vassen, and D. Stöver, Application of Plasma-Sprayed Complex Perovskites as Thermal Barrier Coatings, *J. Therm. Spray Technol.*, 2009. doi:10.1007/s11666-009-9302-9
8. W. Ma, S. Gong, and H. Xu, On Improving the Phase Stability and Thermal Expansion Coefficients of Lanthanum Cerium Oxide Solid Solutions, *Scr. Mater.*, 2006, **54**, p 1505-1508
9. X.Q. Cao, R. Vassen, W. Jungen, S. Schwartz, F. Tietz, and D. Stöver, Thermal Stability of Lanthanum Zirconate Plasma-Sprayed Coating, *J. Am. Ceram. Soc.*, 2001, **84**, p 2086-2090
10. W. Ma, S. Gong, and H. Xu, The Thermal Cycling Behavior of Lanthanum-Cerium Oxide Thermal Barrier Coating Prepared by EB–PVD, *Surf. Coat. Technol.*, 2006, **200**, p 5113-5118
11. H.B. Guo, H. Murakami, and S. Kuroda, Effect of Hollow Spherical Powder Size Distribution on Porosity and Segmentation Cracks in Thermal Barrier Coatings, *J. Am. Ceram. Soc.*, 2006, **89**, p 3797-3804
12. H.B. Guo, S. Kuroda, and H. Murakami, Segmented Thermal Barrier Coatings Produced by Atmospheric Plasma Spraying Hollow Powders, *Thin Solid Films*, 2006, **506**, p 136-139
13. W. Ma, S. Gong, and H. Xu, Novel Thermal Barrier Coatings Based on $La_2Ce_2O_7$/8YSZ Double-Ceramic-Layer Systems Deposited by Electron Beam Physical Vapor Deposition, *Surf. Coat. Technol.*, 2008, **202**, p 2368-2373
14. X. Wang, U. Helmersson, J. Birch, and W. Ni, High Resolution X-Ray Diffraction Mapping Studies on the Domain Structure of $LaAlO_3$ Single Crystal Substrates and Its Influence on $SrTiO_3$ Film Growth, *J. Cryst. Growth*, 1997, **171**, p 401-408
15. F. Brisse and O. Knop, Pyrochlores. II. An Investigation of $La_2Ce_2O_7$ by Neutron Diffraction, *Can. J. Chem.*, 1967, **45**, p 609-615
16. H.B. Guo, R. Vaßen, and D. Stöver, Atmospheric Plasma Sprayed Thick Thermal Barrier Coatings with High Segmentation Crack Density, *Surf. Coat. Technol.*, 2004, **186**, p 353-363
17. H.B. Guo, H. Murakami, and S. Kuroda, Effects of Heat Treatment on Microstructures and Physical Properties of Segmented Thermal Barrier Coatings, *Mater. Trans.*, 2005, **46**, p 1775-1778
18. X. Cao, R. Vassen, W. Fischer, F. Tietz, W. Jungen, and D. Stöver, Lanthanum-Cerium Oxide as a Thermal Barrier Coating for High Temperature Applications, *Adv. Mater.*, 2003, **15**, p 1438-1445
19. R. Taylor, J.R. Brandon, and P. Morrell, Microstructure, Composition and Property Relationships of Plasma-Sprayed Thermal Barrier Coatings, *Surf. Coat. Technol.*, 1992, **50**, p 141-149
20. I.-H. Jung and K.-K. Bae, A Study of The Microstructure of Yttria-Stabilized Zirconia Deposited by Inductively Coupled Plasma Spraying, *J. Therm. Spray Technol.*, 2000, **9**, p 463-477
21. E. Lugscheider, K. Bobzin, and R. Nickel, Application of Multiscale Modeling in the Coating Formation Simulation of APS PYSZ TBCs, *J. Therm. Spray Technol.*, 2006, **15**, p 537-544